The Canadian Mineralogist
Vol. 44, pp. 45-62 (2006)

ALLANITE-(Ce) IN GRANITIC ROCKS FROM JAPAN: GENETIC IMPLICATIONS OF PATTERNS OF REE AND Mn ENRICHMENT

MIHOKO HOSHINO, MITSUYOSHI KIMATA AND MASAHIRO SHIMIZU

Earth Evolution Sciences, Life and Environmental Sciences, The University of Tsukuba, Tennodai 1-1-1, Tsukuba, Ibaraki, 305-8572, Japan

NORIMASA NISHIDA

Chemical Analysis Division, Research Facility Center for Science and Technology, The University of Tsukuba, Tennodai 1-1-1, Tsukuba, Ibaraki, 305-8577, Japan

TAKASHI FUJIWARA

Nippon Chigakukenkyu-kai, Karasuma Demizu, Kamigyo-ku, Kyoto 602-8012, Japan

ABSTRACT

Twenty-two samples of allanite-(Ce) taken from granitic rocks in Japan have been characterized by electron-microprobe analysis. In back-scattered-electron (BSE) images, the allanite-(Ce) is homogeneous or characterized by various types of zoning features: oscillatory, normal or irregular types. Thirteen samples contain appreciable amounts of Mn (0.14–0.59 *apfu*). The Mn-rich crystals (2–6 cm long) are larger than the crystals of Mn-poor allanite-(Ce) (0.5–2 cm long). Samples of the two groups differ considerably from each other in chondrite-normalized REE patterns: Mn-poor allanite-(Ce) is relatively rich in LREE, as is common in igneous allanite, whereas the Mn-rich allanite-(Ce) exhibits an enrichment in the middle rare-earth elements (MREE). The relationship between Mn-rich and Mn-poor allanite-(Ce) is expressed by the coupled substitution Mn^{2+} + (MREE, HREE)$^{3+}$ $\rightleftharpoons$ Ca^{2+} + LREE^{3+}. The presence of Mn-rich allanite-(Ce) in the Japanese island arc, in conjunction with occurrences of Mn-rich and REE-bearing epidote-group minerals in manganese deposits, support a link with subduction-zone processes. The granitic rocks containing Mn-poor allanite-(Ce) belong to the magnetite-series granitic rocks, whereas those containing Mn-rich allanite-(Ce) correspond to the ilmenite series, and seem to have formed from a volatile-enriched magma. Therefore, the Mn content in allanite-(Ce) contains petrogenetic information.

Keywords: allanite-(Ce), rare-earth elements, manganese, chemical zoning, coupled substitution, granitic rocks, origin, crystal size, Japan.

SOMMAIRE

Nous avons caractérisé avec une microsonde électronique la composition chimique de vingt-deux échantillons d'allanite-(Ce) provenant de roches granitiques au Japon. Les images formées par les électrons rétrodiffusés montrent que l'allanite-(Ce) est homogène ou zonée de façon oscillatoire, normale ou irrégulière. Treize échantillons font preuve de quantités importantes de Mn (0.14–0.59 *apfu*). Les cristaux riches en Mn sont plus longs (2–6 cm) que les cristaux à plus faible teneur en Mn (0.5–2 cm). Ces deux groupes d'allanite-(Ce) diffèrent considérablement dans leurs spectres de terres rares normalisés par rapport à une chondrite. L'allanite-(Ce) à faible teneur en Mn est relativement enrichie en terres rares légères (TRL), comme c'est généralement le cas dans l'allanite des roches ignée, tandis que l'allanite-(Ce) riche en Mn montre un enrichissement dans les terres rares moyennes (TRM). La relation entre les deux groupes se décrit par une substitution couplée: Mn^{2+} + (TRM, TR lourdes)$^{3+}$ $\rightleftharpoons$ Ca^{2+} + TRL^{3+}. La présence d'allanite-(Ce) manganifère dans les granites de l'arc insulaire japonais, de même que les indices de minéraux du groupe de l'épidote riches en Mn et en terres rares dans les gisements de manganèse, semblent témoigner d'un lien avec les phénomènes de subduction. Les roches granitiques contenant l'allanite-(Ce) pauvre en Mn font partie de la série de roches granitiques à magnétite, tandis que les roches granitiques contenant l'allanite-(Ce) riche en Mn correspondent à la série à ilménite, et se seraient formées de magmas enrichis en composants volatils. C'est donc dire que la teneur de l'allanite-(Ce) en Mn serait un indicateur de l'origine des roches granitiques.

(Traduit par la Rédaction)

Mots-clés: allanite-(Ce), terres rares, manganèse, zonation chimique, substitution couplée, roches granitiques, origine, taille des cristaux, Japon.

E-mail address: hossy716@arsia.geo.tsukuba.ac.jp

Introduction

Allanite-(Ce), a member of the epidote group of minerals [$A_2 M_3 Si_3 O_{11}O(OH)$, *A*: Ca, Ce; *M*: Al, Fe], is an important host for rare-earth elements (REE), as it occurs as a characteristic accessory mineral in various kinds of rocks: granite, granodiorite, monzonite, syenite, skarns, and felsic volcanic rocks (Deer *et al.* 1986, Gaines *et al.* 1997, Gieré & Sorensen 2004); it also is found in glaucophane schist (Banno 1993). As Ercit (2002) pointed out, there are other species in the allanite subgroup, distinguished on the basis of their REE content: allanite-(La) and allanite-(Y). In most cases, allanite incorporates Th and U. Decay of these elements causes metamictization (Gieré & Sorensen 2004).

In Japan, allanite-(Ce), having an idealized formula $(Ce,Ca,Y)_2(Al,Fe^{3+})_3(SiO_4)_3(OH)$, most commonly occurs in granite, granitic pegmatite, gabbroic pegmatite, monzonite pegmatite and granodiorite (Omori & Hasegawa 1956, Nagashima & Nagashima 1960, Hasegawa 1957, 1958, 1959, 1960, 1961), and rarely in metamorphic rocks (Sakai *et al.* 1984, Banno 1993). Until the middle 1990s, the multiplicity of characteristic X-ray lines for REE precluded accurate electron- microprobe analysis (EPMA) of REE-bearing minerals. Development of better methods through careful measurement of these X-ray lines has improved the REE data obtained by EPMA (*e.g.*, Reed & Buckley 1998, Nishida *et al.* 1999). Moreover, back-scattered-electron (BSE) images of allanite grains typically show the presence of zoning controlled by the abundance of light rare-earth elements (LREE), Fe, Th, and U (*e.g.*, Sorensen 1991, Carcangiu *et al.* 1997, Catlos *et al.* 2000). However, almost all chemical compositions of allanite from granitic rocks in Japan were reported prior to the effective use of EPMA. The exception is the allanite from granitic rocks documented by Suzuki *et al.* (1990). Early detailed studies (Hasegawa 1960) confirmed that the Mn content in allanite from Japan are generally higher than those from other countries in the region. High contents of manganese are generally associated with low Ca contents, and the sum of (Mn + Ca) ions is approximately constant in allanite (Deer *et al.* 1986).

Our purpose here is document and interpret the chemical compositions of allanite from granitic rocks in Japan and associated with the Japanese island arc in comparison with those from other regions.

TABLE 1. STANDARD MATERIALS USED FOR WAVELENGTH-DISPERSION ELECTRON-MICROPROBE ANALYSIS

Standard	Chemical composition (wt%)			
Y	SiO_2 (54.3)	Al_2O_3 (12.7)	CaO (20.5)	Y_2O_3 (11.8)
La	SiO_2 (54.3)	Al_2O_3 (12.7)	CaO (20.6)	La_2O_3 (11.5)
Ce	SiO_2 (54.2)	Al_2O_3 (12.8)	CaO (20.4)	Ce_2O_3 (11.9)
Pr	SiO_2 (54.0)	Al_2O_3 (12.7)	CaO (20.6)	Pr_2O_3 (12.2)
Nd	SiO_2 (54.4)	Al_2O_3 (12.8)	CaO (20.8)	Nd_2O_3 (11.8)
Sm	SiO_2 (54.8)	Al_2O_3 (12.9)	CaO (20.8)	Sm_2O_3 (11.2)
Gd	SiO_2 (54.8)	Al_2O_3 (12.1)	CaO (20.7)	Gd_2O_3 (12.1)
Tb	SiO_2 (54.6)	Al_2O_3 (12.6)	CaO (20.2)	Tb_2O_3 (11.9)
Dy	SiO_2 (54.7)	Al_2O_3 (12.5)	CaO (20.6)	Dy_2O_3 (12.0)
Er	SiO_2 (54.6)	Al_2O_3 (12.6)	CaO (20.5)	Er_2O_3 (11.9)
Tm	SiO_2 (54.8)	Al_2O_3 (12.4)	CaO (20.3)	Tm_2O_3 (11.9)
Yb	SiO_2 (54.7)	Al_2O_3 (12.6)	CaO (20.7)	Yb_2O_3 (12.0)

All standards are from P & H Development Ltd., U.K.

Analytical Methods

The chemical composition of allanite were determined with a JEOL JXA–8621 electron microprobe equipped with three wavelength-dispersion spectrometers (WDS) at the Chemical Analysis Division, University of Tsukuba. Chemical zoning of allanite was recorded with high resolution using BSE images. Qualitative analyses were made using 25 kV accelerating potential and 2.5×10^{-7} A beam current. New methods of correction for overlap between REE have been developed by Reed & Buckley (1998) and Nishida *et al.* (1999). We adopted the latter method. Quantitative analyses of allanite for major elements were carried out using an accelerating voltage of 25 kV and a beam current 1.0×10^{-8} A. Concentrations of the REE were measured at 25 kV with a beam current 5.0×10^{-8} A. X-ray intensities for Y, La, Ce, Nd, Er, Tb, Tm, Yb were determined using the $L\alpha_1$ X-ray lines, whereas the intensities for Pr, Sm, Gd and Dy peaks were measured using the $L\beta_1$ lines. For REE standards, we used synthetic Ca–Al silicate glasses containing each REE, which are available from P & H Development Ltd. (Table 1). All the data were corrected with a ZAF matrix-correction program. The locations and descriptions of occurrences of the samples analyzed are given in Table 2.

Results

Zoning types and chemical compositions of allanite

Grains of allanite from granitic rocks are known to have three types of optical zoning, as revealed in BSE images: (1) oscillatory zoning (*e.g.*, Deer *et al.* 1986, Buda & Nagy 1995, Dahlquist 2001), (2) normal growth-induced magmatic zoning (Poitrasson 2002, Oberli *et al.* 2004, Gieré & Sorensen 2004), and (3) complicated internal zoning consisting of a patchwork of domains variable in brightness (Petrík *et al.* 1995). However, the chemical zoning for most of the allanite samples presently examined has been defined as of an irregular type (Table 2, Figs. 1b, d, e, f, q, r, s, t, u), although the three types of zoning present (Figs. 1b, s, u) are broadly similar in texture to the complicated pattern of internal zoning (Petrík *et al.* 1995). Under the polarizing microscope, the chemical zones within each of the allanite crystals show simultaneous extinction.

TABLE 2. MINERALOGICAL AND PETROGRAPHIC DATA FOR ALLANITE-(Ce) FROM GRANITIC ROCKS, JAPAN

#	Morphology	Type of zoning	Mn (*apfu*)**	Crystal size (cm)	Host rock***	Series †	Location	Ref. ‡
a	prismatic euhedral	magmatic	0.037-0.043	0.3 × 0.3 × 0.5	GP	magnetite	Miyamori, Iwate	1
b	anhedral	irregular	0.564-0.624	2.5 × 2.5 × 5.0	GP	ilmenite	Suishyoyama, Fukushima	2
c	prismatic euhedral	magmatic	0.054-0.060	0.5 × 0.5 × 1.5	GP	ilmenite	Kitatosawa, Fukushima	2
d	dendritic	irregular	0.099-0.153	-	GP	ilmenite	Shiodaira, Fukushima	1
e	subhedral	irregular	0.215-0.223	0.6 × 0.6 × 2.5	GP	ilmenite	Utsumine, Fukushima	1
f	anhedral	irregular	0.173-0.177	2.0 × 2.0 × 3.5	GP	ilmenite	Matsuzuka, Fukushima	-§
g	subhedral	homog.	0.346-0.372	1.0 × 1.5 × 2.0	GP	ilmenite	Shimo-ono, Ibaraki	1
h	subhedral	mixture*	0.525-0.605	1.5 × 1.5 × 4.5	GP	ilmenite	Haguri, Shiga	1
i	prismatic euhedral	oscillatory	0.019-0.070	0.1 × 0.1 × 0.5	G	magnetite	Omiyadani, Shiga	-
j	prismatic euhedral	homog.	0.065-0.079	0.5 × 0.5 × 1.0	GP	magnetite	Daibosatsu, Yamanashi	1
k	anhedral	magmatic	0.040-0.112	0.2 × 0.2 × 0.5	G	magnetite	Nagatejima, Ishikawa	1
l	dendritic	oscillatory	0.049-0.061	-	GP	magnetite	Hirono, Kyoto	-
m	prismatic euhedral	mixture	0.265-0.304	0.5 × 0.5 × 2.0	GP	magnetite	Ōro, Kyoto	1, 3
n	prismatic euhedral	oscillatory	0.014-0.069	0.3 × 0.3 × 1.0	G	magnetite	Daimonjiyama, Kyoto	1
o	anhedral	magmatic	0.157-0.165	3.5 × 3.5 × 4.5	GP	ilmenite	Kamo, Kyoto	-
p	anhedral	magmatic	0.079-0.088	0.5 × 0.5 × 1.5	GP	ilmenite	Daian, Mie	-
q	prismatic euhedral	irregular	0.144-0.168	1.5 × 1.5 × 5.5	GP	ilmenite	Fukudayama, Mie	1
r	anhedral	irregular	0.289-0.364	0.5 × 0.3 × 2.5	GP	ilmenite	Geino, Mie	-
s	anhedral	irregular	0.363-0.455	3.0 × 2.5 × 6.0	GP	ilmenite	Kanayama, Kagawa	4, 5
t	anhedral	irregular	0.307-0.364	3.5 × 3.5 × 5.0	GP	ilmenite	Tateiwa, Ehime	1, 5
u	anhedral	irregular	0.245-0.275	1.0 × 1.0 × 3.0	GP	ilmenite	Tamagawa, Ehime	5
v	subhedral	magmatic	0.112-0.118	0.5 × 0.4 × 2.0	GP	magnetite	Kaho, Fukuoka	-

* Mixture represents a combination of magmatic and irregular types. ** The allanite grains can be divided into Mn-rich type (more than 0.14 *apfu* Mn) and Mn-poor type (less than 0.14 *apfu* Mn). See Table 3-7, Figures 2 and 3. *** Host-rock codes: GP: granitic pegmatite, G: granite. † Granitic rocks are classified according to Ishihara (1977, 1981), Shibata & Ishihara (1979) and Takagi (2004). ‡ Reference for locality: 1 Nagashima & Nagashima (1960), (2) Hasegawa (1957), (3) Yamada *et al.* (1980), (4) Hasegawa (1958), and (5) Hasegawa (1959). -§: no reference.

Representative compositions of allanite are provided in Tables 3–7. The EPMA data demonstrate that Ce is predominant over other REE in all allanite grains studied here; they are thus identified as allanite-(Ce). Different degrees of metamictization are exhibited as a result of variability in radionuclide content (particularly Th), as confirmed by X-ray-diffraction patterns. A single smooth hump is produced by diffuse scattering of X rays by the aperiodic material; most of the allanite samples studied are in a slightly metamict or non-metamict state, except for those from Miyanomori, Shimo-ono, Kamo and Fukudayama (Hoshino *et al.* 2005). The WDS analytical results presented here show that Eu is below the detection limit in all samples. Of the 22 samples examined, thirteen contain appreciable amounts of Mn (0.14–0.59 atoms per formula unit, *apfu*). The samples may be divided into Mn-rich (Mn > 0.14 *apfu*) and Mn-poor allanite (Mn < 0.14 *apfu*) (Tables 2–7, Figs. 2, 3). Most of the allanite-(Ce) samples exhibit A-site vacancies to varying degrees (Table 3–7). The mechanism of incorporation of vacancies will be discussed later. Their structural formulae were first calculated by normalizing the $(M + T)$ cations to 6 *apfu*; this normalization is followed by varying Fe^{2+}/Fe^{3+} until the total number of positive charges equals 25 (Ercit 2002). The assignment of cations based on charge balance is summarized in Tables 3–7.

The Mn-bearing allanite-(Ce) is crystal-chemically different from androsite, REE-bearing piemontite and khristovite, as clearly distinguished in an $\Sigma REE - (Fe^{2+} + Fe^{3+}) - (Mn^{2+} + Mn^{3+})$ diagram (Fig. 2). Compilation of the present and previous data on allanites from granitic rocks (Fig. 3) shows that a general decrease in Ca can be observed with increasing total Mn. However, a correct understanding of this observation involves the distribution of Mn between the *A* and *M* sites. Therefore, a trace of Mn^{2+} is interpreted to occupy the *M*3 site in our samples. Concerning the other Mn-bearing epidote-group minerals, REE-bearing piemontite shows extensive solid-solution toward allanite (Bonazzi *et al.* 1992, Bonazzi & Menchetti 1994, Bermanec *et al.* 1994) as a result of the coupled substitution $Ca^{2+} + Mn^{3+} \rightleftharpoons REE^{3+} + Fe^{2+}$ (Gieré & Sorensen 2004). On the other hand, khristovite (Sokolova *et al.* 1991) contains Mn^{2+} rather than Mg at the *M*3 site (Gieré & Sorensen 2004). This Mn^{2+} site-preference is consistent with the result obtained from the present analyses.

The chemical zoning observed in the allanite grains seems to be caused by variations in Th, Fe^{2+}, Fe^{3+}, Mn, and REE contents (Tables 3–7). In the BSE images, Mn-poor allanite displays either an almost

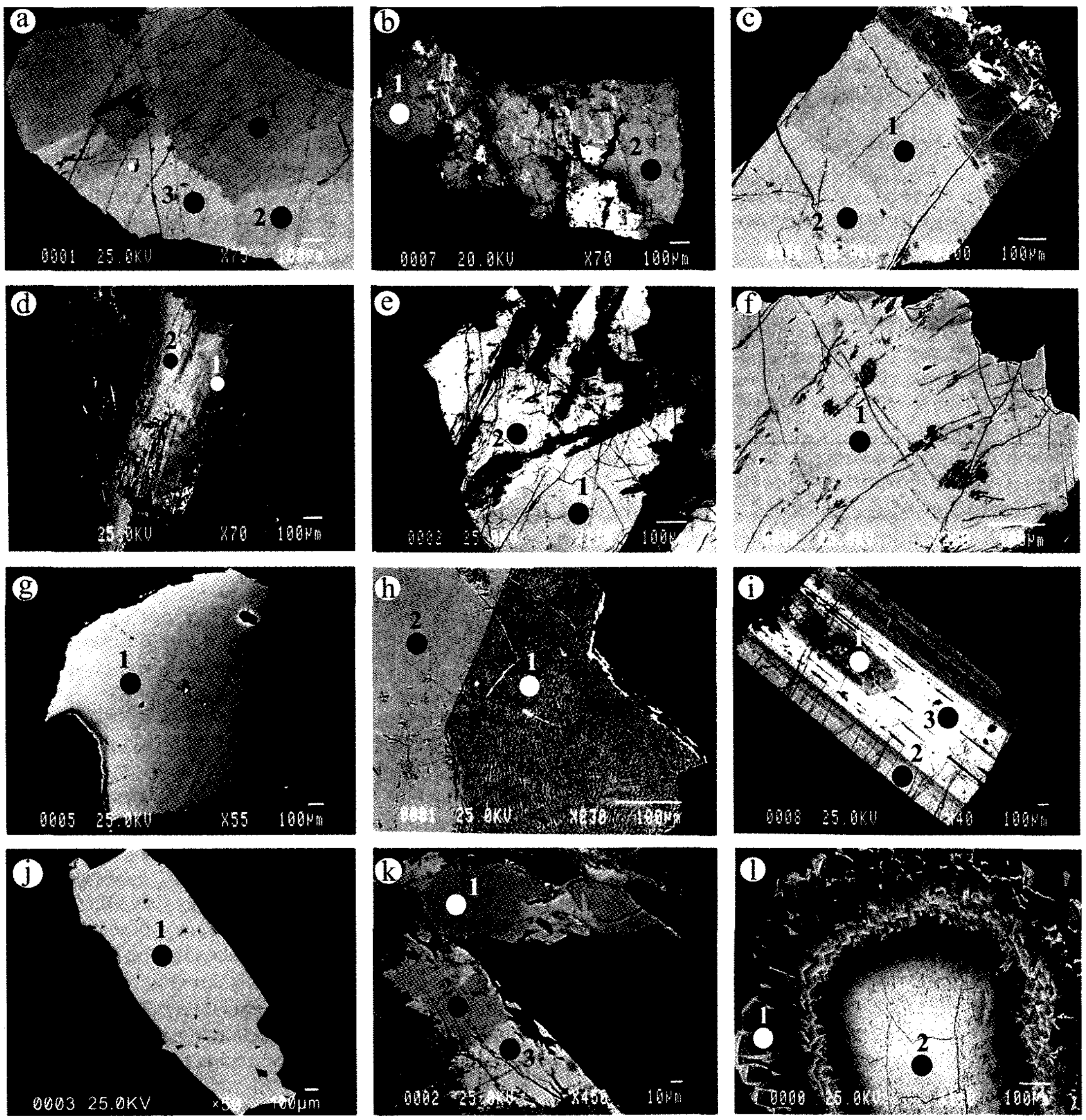

homogeneous distribution of elements or an oscillatory magmatic zoning, whereas most Mn-rich samples exhibit irregular zoning. Moreover, Mn-poor allanite tends to have a euhedral or subhedral shape, in contrast with the Mn-rich grains, which are mostly anhedral crystals (Table 2).

Discussion

A-site vacancies in allanite

Although the *A* sites of some allanties may be partially vacant, it is difficult to document the presence of vacancies due to the chemical complexity of the mineral, and especially the uncertainties of the calculation of Fe^{2+}/Fe^{3+} from electron-microprobe data (Ercit 2002, Gieré & Sorensen 2004). However, corroborative evidence exists to support the idea that vacancies may occur at the *A* site of allanite and related minerals. In conjunction with electron-microprobe data, the structural refinement of khristovite-(Ce) yielded a considerable proportion of vacancies at the *A* site, as is evident from the refined formula $(Ca_{0.6}La_{0.2}\square_{0.2})$ $(Ce_{0.5}La_{0.12}Nd_{0.15}Dy_{0.10}Pr_{0.05}Sm_{0.02}\square_{0.07})$ $(Mg_{0.40}Fe_{0.15}Cr_{0.12}Ti_{0.12}V_{0.09}Al_{0.12})AlMn$ $(SiO_4)(Si_2O_7)(OH)(F_{0.63}O_{0.37})$ (Sokolova *et al.* 1991). In addition, from their chemical

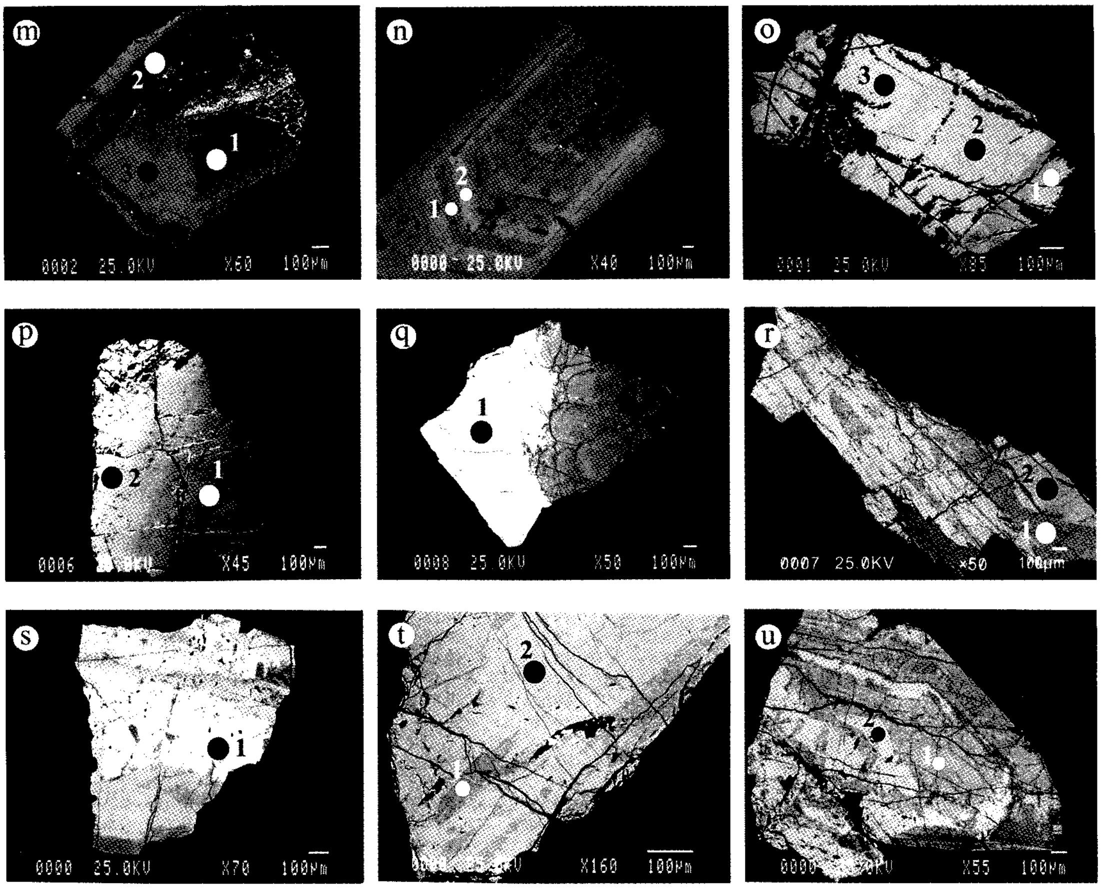

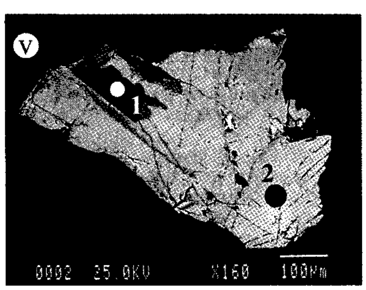

FIG. 1. Back-scattered-electron images showing representative textures of the allanite-(Ce). Localities: (a) Miyamori, (b) Suishyoyama, (c) Kitatosawa, (d) Shiodaira, (e) Utsumine, (f) Matsuzuka, (g) Shimo-ono, (h) Haguri, (i) Omiyadani, (j) Daibosatsu, (k) Nagatejima, (l) Hirono, (m) Ōro, (n) Daimonjiyama, (o) Kamo, (p) Daian, (q) Fukudayama, (r) Geino, (s) Kanayama, (t) Tateiwa, (u) Tamagawa, and (v) Kaho. The numbered solid circles denote the locations of electron-microprobe analyses, corresponding to the numbers in Tables 3–7.

compositions, Peterson & MacFarlane (1993) also estimated varying degrees of vacancy at the *A* site of most of the allanite samples they investigated from granitic rocks and calcite veins in the Grenville Province, Ontario, Canada. Furthermore, these vacancies were interpreted as a result of an omission-type substitution: $3Ca^{2+} = 2REE^{3+} + \square$, where the proportion of the vacancy ranges from 0.059 to 0.439 (Peterson & MacFarlane 1993). Our thirteen samples of allanite incorporate appreciable amounts of Mn at the *A* sites. Therefore, the low *A*-site occupancies for some of the samples suggest the following mechanism of incorporation of the vacancy with the maintenance of charge neutrality: $3(Ca, Mn)^{2+} = 2REE^{3+} + \square$ (Fig. 4).

The behavior of REE and Mn in allanite from Japan

Examination of chemical compositions of allanite from granitic rocks in Japan, as explained in the preceding section, leads to the division into Mn-poor and Mn-rich types (Tables 2–7, Figs. 2, 3). The observation that Mn-rich and Mn-poor compositions do not

TABLE 3. REPRESENTATIVE COMPOSITIONS OF ALLANITE-(Ce) FROM MIYAMORI, SUISHYOYAMA, KITATOSAWA AND SHIODAIRA LOCALITIES

Sample	a) Miyamori			b) Suishyoyama		c) Kitatosawa		d) Shiodaira	
Location	1	2	3	1	2	1	2	1	2
n	5	5	5	5	6	5	5	3	3
SiO_2	33.93(0.50)	33.80(0.30)	33.51(0.15)	31.65(0.28)	31.21(0.51)	32.63(0.27)	32.44(0.29)	33.10(0.11)	31.93(0.02)
TiO_2	1.26(0.03)	1.20(0.03)	1.54(0.02)	<0.003	<0.003	0.88(0.02)	0.92(0.02)	0.04(0.00)	0.10(0.02)
Al_2O_3	15.07(0.19)	14.85(0.09)	14.22(0.08)	15.36(0.13)	15.31(0.04)	17.64(0.06)	17.45(0.04)	21.21(0.01)	20.32(0.03)
Fe_2O_3	11.21(0.11)	11.30(0.10)	11.55(0.06)	9.93(0.19)	9.30(0.11)	11.60(0.09)	11.55(0.16)	8.76(0.13)	9.56(0.02)
FeO	4.10(0.11)	4.34(0.10)	4.34(0.06)	5.40(0.05)	7.16(0.10)	3.76(0.08)	3.84(0.14)	3.65(0.13)	3.51(0.02)
MnO	0.54(0.01)	0.51(0.01)	0.54(0.00)	7.00(0.05)	7.64(0.06)	0.74(0.02)	0.76(0.01)	1.42(0.05)	1.94(0.07)
MgO	1.35(0.02)	1.27(0.12)	1.52(0.02)	<0.002	<0.002	0.37(0.01)	0.36(0.01)	0.10(0.01)	0.15(0.01)
CaO	11.79(0.03)	11.47(0.04)	11.12(0.08)	3.59(0.06)	3.67(0.02)	11.83(0.06)	11.90(0.02)	12.47(0.05)	11.02(0.01)
Sc_2O_3	<0.002	<0.002	<0.002	<0.002	<0.002	<0.002	<0.002	<0.002	<0.002
Y_2O_3	<0.10	<0.10	<0.10	1.61(0.06)	1.56(0.02)	0.67(0.04)	0.70(0.03)	<0.10	<0.10
La_2O_3	5.14(0.08)	5.28(0.12)	5.68(0.06)	2.75(0.10)	3.00(0.00)	4.30(0.09)	4.14(0.08)	2.63(0.03)	3.16(0.04)
Ce_2O_3	7.65(0.05)	7.97(0.07)	8.16(0.13)	7.38(0.24)	7.74(0.27)	7.02(0.15)	6.80(0.06)	6.01(0.01)	6.10(0.44)
Pr_2O_3	1.29(0.07)	1.26(0.04)	1.30(0.01)	1.45(0.06)	1.55(0.04)	1.11(0.05)	1.08(0.05)	1.18(0.01)	1.34(0.06)
Nd_2O_3	3.21(0.03)	3.22(0.00)	3.26(0.03)	4.93(0.06)	5.39(0.00)	3.55(0.02)	3.56(0.07)	3.87(0.01)	4.25(0.06)
Sm_2O_3	0.82(0.02)	0.80(0.02)	0.81(0.01)	1.79(0.03)	1.86(0.04)	0.70(0.01)	0.76(0.08)	2.85(0.07)	3.05(0.01)
Gd_2O_3	<0.22	<0.22	<0.22	1.46(0.06)	1.55(0.00)	0.76(0.01)	0.79(0.04)	2.09(0.04)	1.98(0.04)
Tb_2O_3	<0.15	<0.15	<0.15	<0.15	<0.15	<0.15	<0.15	<0.15	<0.15
Dy_2O_3	<0.22	<0.22	<0.22	<0.22	<0.22	<0.22	<0.22	<0.22	<0.22
Er_2O_3	<0.13	<0.13	<0.13	<0.13	<0.13	<0.13	<0.13	<0.13	<0.13
Tm_2O_3	<0.12	<0.12	<0.12	<0.12	<0.12	<0.12	<0.12	<0.12	<0.12
Yb_2O_3	<0.11	<0.11	<0.11	<0.11	<0.11	<0.11	<0.11	<0.11	<0.11
ThO_2	2.41(0.04)	2.65(0.04)	2.75(0.08)	1.62(0.04)	1.48(0.02)	1.48(0.00)	1.40(0.02)	0.24(0.00)	0.28(0.02)
Na_2O	<0.04	<0.04	<0.04	<0.04	<0.04	<0.04	<0.04	<0.04	<0.04
K_2O	<0.01	<0.01	<0.01	<0.01	<0.01	<0.01	<0.01	<0.01	<0.01
Total	99.77	99.92	100.30	95.92	98.42	99.04	98.45	99.62	98.69
Si	3.060(0.040)	3.061(0.065)	3.046(0.048)	3.076(0.033)	3.009(0.044)	2.944(0.022)	2.943(0.024)	2.924(0.019)	2.889(0.009)
^{T}Al	0.000	0.000	0.000	0.000	0.000	0.056(0.000)	0.057(0.000)	0.076(0.000)	0.111(0.000)
Total T	3.060	3.061	3.046	3.076	3.009	3.000	3.000	3.000	3.000
Ti	0.085(0.024)	0.082(0.004)	0.105(0.002)	0.000	0.000	0.060(0.003)	0.063(0.002)	0.002(0.000)	0.007(0.002)
^{M}Al	1.603(0.013)	1.586(0.015)	1.524(0.007)	1.759(0.018)	1.739(0.021)	1.819(0.014)	1.809(0.012)	2.132(0.003)	2.056(0.009)
Fe^{3+}	0.761(0.017)	0.770(0.014)	0.790(0.007)	0.726(0.010)	0.577(0.036)	0.788(0.014)	0.788(0.022)	0.582(0.007)	0.651(0.001)
Fe^{2+}	0.309(0.017)	0.329(0.014)	0.330(0.007)	0.439(0.011)	0.675(0.039)	0.283(0.016)	0.290(0.024)	0.270(0.007)	0.266(0.001)
^{M}Mn	0.000	0.000	0.000	0.000	0.000	0.000	0.000	0.000	0.000
Mg	0.182(0.005)	0.172(0.034)	0.205(0.004)	0.000	0.000	0.050(0.002)	0.050(0.002)	0.014(0.003)	0.020(0.003)
Total M	2.940	2.939	2.954	2.924	2.991	3.000	3.000	3.000	3.000
Ca	1.139(0.010)	1.113(0.009)	1.083(0.013)	0.374(0.013)	0.379(0.023)	1.144(0.020)	1.157(0.008)	1.180(0.009)	1.068(0.003)
^{A}Mn	0.041(0.002)	0.039(0.002)	0.042(0.001)	0.576(0.012)	0.624(0.000)	0.057(0.003)	0.058(0.002)	0.106(0.007)	0.149(0.004)
Sc	0.000	0.000	0.000	0.000	0.000	0.000	0.000	0.000	0.000
Y	0.000	0.000	0.000	0.083(0.006)	0.080(0.003)	0.032(0.004)	0.034(0.003)	0.000	0.000
La	0.171(0.009)	0.176(0.008)	0.190(0.003)	0.099(0.008)	0.107(0.002)	0.143(0.006)	0.139(0.007)	0.086(0.002)	0.105(0.003)
Ce	0.253(0.003)	0.264(0.006)	0.272(0.007)	0.263(0.017)	0.273(0.015)	0.232(0.008)	0.226(0.004)	0.194(0.001)	0.202(0.028)
Pr	0.043(0.005)	0.042(0.003)	0.043(0.001)	0.051(0.004)	0.054(0.003)	0.036(0.004)	0.036(0.003)	0.038(0.000)	0.044(0.004)
Nd	0.103(0.001)	0.104(0.000)	0.106(0.001)	0.171(0.003)	0.186(0.003)	0.114(0.002)	0.115(0.004)	0.122(0.000)	0.137(0.004)
Sm	0.026(0.001)	0.025(0.002)	0.025(0.001)	0.060(0.003)	0.062(0.002)	0.022(0.000)	0.024(0.005)	0.087(0.004)	0.095(0.001)
Gd	0.000	0.000	0.000	0.047(0.004)	0.050(0.001)	0.023(0.001)	0.024(0.003)	0.061(0.002)	0.058(0.003)
Tb	0.000	0.000	0.000	0.000	0.000	0.000	0.000	0.000	0.000
Dy	0.000	0.000	0.000	0.000	0.000	0.000	0.000	0.000	0.000
Er	0.000	0.000	0.000	0.000	0.000	0.000	0.000	0.000	0.000
Tm	0.000	0.000	0.000	0.000	0.000	0.000	0.000	0.000	0.000
Yb	0.000	0.000	0.000	0.000	0.000	0.000	0.000	0.000	0.000
Th	0.049(0.001)	0.055(0.002)	0.057(0.003)	0.036(0.002)	0.032(0.000)	0.030(0.000)	0.029(0.001)	0.005(0.003)	0.006(0.003)
Na	0.000	0.000	0.000	0.000	0.000	0.000	0.000	0.000	0.000
K	0.000	0.000	0.000	0.000	0.000	0.000	0.000	0.000	0.000
Total A	1.825	1.818	1.818	1.760	1.847	1.833	1.842	1.879	1.864

See Figures 1a-d for spot locations. *n*: number of microprobe points. Number in parentheses is standard deviation. The compositions are first reported in wt%, then the proportion of cations is reported in atoms per formula unit (*apfu*).

TABLE 4. REPRESENTATIVE COMPOSITIONS OF ALLANITE-(Ce) FROM UTSUMINE, MATSUZUKA, SHIMO-ONO, HAGURI AND OMIYADANI

Sample	e) Utsumine		f) Matsuzuka	g) Shimo-ono	h) Haguri		i) Omiyadani		
Location	1	2	1	1	1	2	1	2	3
n	5	5	8	8	5	5	3	5	3
SiO_2	33.32(0.21)	33.01(0.26)	33.23(0.94)	32.43(0.64)	31.44(0.20)	31.23(0.12)	33.77(0.21)	34.18(0.00)	33.53(0.23)
TiO_2	0.70(0.04)	0.84(0.04)	0.29(0.01)	0.80(0.06)	<0.003	<0.003	1.03(0.01)	1.10(0.02)	0.47(0.02)
Al_2O_3	16.07(0.07)	15.39(0.09)	18.21(0.08)	14.50(0.12)	15.96(0.07)	15.83(0.11)	17.66(0.55)	18.27(0.08)	18.02(0.24)
Fe_2O_3	7.80(0.10)	7.50(0.10)	12.44(0.08)	8.64(0.18)	10.99(0.16)	12.60(0.28)	12.61(0.88)	8.63(0.67)	11.76(0.12)
FeO	5.95(0.11)	7.01(0.09)	2.20(0.07)	8.47(0.16)	5.35(0.14)	4.35(0.38)	1.16(0.79)	3.62(0.60)	2.45(0.12)
MnO	2.80(0.01)	2.79(0.02)	2.28(0.05)	4.52(0.01)	6.61(0.03)	7.31(0.12)	0.25(0.00)	0.54(0.01)	0.89(0.01)
MgO	0.57(0.11)	0.65(0.04)	<0.002	0.15(0.00)	<0.002	<0.002	1.05(0.21)	0.73(0.11)	0.50(0.04)
CaO	10.67(0.03)	10.61(0.08)	9.25(0.08)	7.76(0.03)	3.13(0.04)	2.33(0.02)	10.29(0.46)	11.38(0.06)	9.52(0.13)
Sc_2O_3	0.44(0.01)	0.50(0.06)	0.12(0.01)	<0.002	<0.002	<0.002	<0.002	<0.002	<0.002
Y_2O_3	0.54(0.04)	0.43(0.04)	<0.10	1.13(0.01)	1.93(0.05)	1.90(0.09)	<0.10	<0.10	<0.10
La_2O_3	3.03(0.03)	3.30(0.07)	2.72(0.11)	2.39(0.01)	2.28(0.07)	2.26(0.14)	6.66(0.37)	5.54(0.05)	6.08(0.11)
Ce_2O_3	6.77(0.09)	6.86(0.34)	6.07(0.45)	5.68(0.00)	6.65(0.05)	6.66(0.12)	9.35(0.34)	8.12(0.09)	9.03(0.07)
Pr_2O_3	1.40(0.02)	1.38(0.12)	1.28(0.02)	1.27(0.00)	1.48(0.05)	1.52(0.06)	1.28(0.05)	1.20(0.03)	1.42(0.03)
Nd_2O_3	4.22(0.06)	4.22(0.03)	4.89(0.05)	5.30(0.01)	6.20(0.12)	6.26(0.16)	3.37(0.03)	3.42(0.01)	4.13(0.09)
Sm_2O_3	1.67(0.03)	1.55(0.04)	1.36(0.01)	1.93(0.00)	2.87(0.09)	2.88(0.14)	0.56(0.01)	0.64(0.01)	0.80(0.04)
Gd_2O_3	1.15(0.03)	1.02(0.05)	1.08(0.01)	1.46(0.00)	2.08(0.06)	2.21(0.05)	<0.22	<0.22	<0.22
Tb_2O_3	<0.15	<0.15	<0.15	<0.15	<0.15	<0.15	<0.15	<0.15	<0.15
Dy_2O_3	<0.22	<0.22	0.40(0.01)	0.54(0.00)	0.86(0.03)	0.84(0.06)	<0.22	<0.22	<0.22
Er_2O_3	<0.13	<0.13	0.21(0.01)	<0.13	<0.13	<0.13	<0.13	<0.13	<0.13
Tm_2O_3	<0.12	<0.12	<0.12	<0.12	<0.12	<0.12	<0.12	<0.12	<0.12
Yb_2O_3	<0.11	<0.11	0.18(0.02)	<0.11	<0.11	<0.11	<0.11	<0.11	<0.11
ThO_2	1.55(0.02)	1.83(0.05)	2.19(0.01)	3.11(0.07)	1.76(0.05)	1.48(0.08)	0.97(0.02)	1.59(0.02)	1.61(0.10)
Na_2O	<0.04	<0.04	<0.04	<0.04	<0.04	<0.04	<0.04	<0.04	<0.04
K_2O	<0.01	<0.01	<0.01	<0.01	<0.01	<0.01	<0.01	<0.01	<0.01
Total	98.65	98.89	98.40	100.08	99.59	99.66	100.01	98.96	100.21
Si	3.060(0.060)	3.050(0.060)	3.015(0.093)	3.044(0.057)	2.994(0.018)	2.974(0.040)	3.007(0.010)	3.054(0.040)	3.013(0.006)
^{T}Al	0.000	0.000	0.000	0.000	0.006(0.000)	0.026(0.000)	0.000	0.000	0.000
Total *T*	3.060	3.050	3.015	3.044	3.000	3.000	3.007	3.054	3.013
Ti	0.049(0.005)	0.058(0.006)	0.020(0.092)	0.056(0.009)	0.000	0.000	0.069(0.002)	0.074(0.004)	0.032(0.003)
^{M}Al	1.739(0.008)	1.676(0.016)	1.948(0.062)	1.604(0.016)	1.786(0.016)	1.751(0.007)	1.853(0.088)	1.924(0.003)	1.908(0.026)
Fe^{3+}	0.539(0.012)	0.522(0.059)	0.850(0.028)	0.610(0.029)	0.788(0.012)	0.903(0.077)	0.845(0.127)	0.580(0.077)	0.795(0.019)
Fe^{2+}	0.457(0.012)	0.542(0.060)	0.167(0.030)	0.665(0.032)	0.426(0.014)	0.346(0.050)	0.086(0.137)	0.271(0.083)	0.184(0.021)
^{M}Mn	0.078(0.000)	0.062(0.000)	0.000	0.000	0.000	0.000	0.000	0.000	0.000
Mg	0.078(0.031)	0.090(0.010)	0.000	0.021(0.004)	0.000	0.000	0.139(0.054)	0.097(0.029)	0.067(0.012)
Total *M*	2.940	2.950	2.985	2.956	3.000	3.000	2.993	2.946	2.987
Ca	1.050(0.009)	1.050(0.014)	0.899(0.019)	0.780(0.032)	0.319(0.009)	0.238(0.000)	0.982(0.074)	1.090(0.000)	0.917(0.014)
^{A}Mn	0.140(0.003)	0.157(0.004)	0.175(0.002)	0.359(0.013)	0.533(0.008)	0.590(0.015)	0.019(0.000)	0.041(0.001)	0.068(0.002)
Sc	0.035(0.001)	0.040(0.009)	0.009(0.000)	0.000	0.000	0.000	0.000	0.000	0.000
Y	0.026(0.004)	0.021(0.004)	0.000	0.056(0.009)	0.098(0.006)	0.096(0.009)	0.000	0.000	0.000
La	0.102(0.002)	0.112(0.006)	0.091(0.009)	0.083(0.006)	0.080(0.005)	0.079(0.009)	0.219(0.029)	0.183(0.006)	0.202(0.005)
Ce	0.227(0.006)	0.232(0.022)	0.202(0.031)	0.195(0.004)	0.232(0.004)	0.232(0.006)	0.305(0.028)	0.266(0.009)	0.297(0.008)
Pr	0.047(0.001)	0.046(0.008)	0.042(0.003)	0.043(0.003)	0.051(0.004)	0.053(0.005)	0.042(0.004)	0.039(0.002)	0.046(0.002)
Nd	0.138(0.004)	0.139(0.003)	0.158(0.001)	0.178(0.005)	0.211(0.008)	0.213(0.011)	0.107(0.004)	0.109(0.002)	0.133(0.008)
Sm	0.053(0.002)	0.049(0.003)	0.043(0.002)	0.062(0.003)	0.094(0.005)	0.095(0.011)	0.017(0.001)	0.020(0.001)	0.025(0.002)
Gd	0.035(0.002)	0.031(0.003)	0.032(0.001)	0.045(0.003)	0.066(0.004)	0.070(0.004)	0.000	0.000	0.000
Tb	0.000	0.000	0.000	0.000	0.000	0.000	0.000	0.000	0.000
Dy	0.000	0.000	0.012(0.001)	0.016(0.004)	0.026(0.002)	0.026(0.004)	0.000	0.000	0.000
Er	0.000	0.000	0.006(0.001)	0.000	0.000	0.000	0.000	0.000	0.000
Tm	0.000	0.000	0.000	0.000	0.000	0.000	0.000	0.000	0.000
Yb	0.000	0.000	0.005(0.002)	0.000	0.000	0.000	0.000	0.000	0.000
Th	0.032(0.001)	0.038(0.002)	0.045(0.019)	0.066(0.007)	0.038(0.002)	0.032(0.004)	0.020(0.001)	0.032(0.001)	0.033(0.005)
Na	0.000	0.000	0.000	0.000	0.000	0.000	0.000	0.000	0.000
K	0.000	0.000	0.000	0.000	0.000	0.000	0.000	0.000	0.000
Total *A*	1.885	1.915	1.719	1.883	1.748	1.724	1.711	1.780	1.721

See Figures 1e-i for spot locations. *n*: number of microprobe points. Number in parentheses is standard deviation. The compositions are first reported in wt%, then the proportion of cations is reported in atoms per formula unit (*apfu*).

TABLE 5. REPRESENTATIVE COMPOSITIONS OF ALLANITE-(Ce) FROM DAIBOSATSU, NAGATEJIMA, HIRONO AND ORO

Sample	j) Daibosatsu	k) Nagatejima			l) Hirono		m) Ōro		
Location	1	1	2	3	1*	2	1	2	3
n	8	3	3	3	3	8	5	5	5
SiO_2	31.05(0.15)	35.58(0.74)	33.12(1.54)	35.22(0.94)	37.98(0.25)	33.74(0.48)	32.96(0.34)	31.58(0.97)	31.21(0.23)
TiO_2	1.11(0.05)	0.56(0.03)	0.68(0.05)	0.58(0.01)	0.29(0.03)	0.82(0.12)	1.92(0.01)	1.64(0.05)	1.54(0.01)
Al_2O_3	14.53(0.20)	18.41(0.00)	17.77(0.29)	16.13(0.21)	23.03(0.30)	17.07(0.48)	13.32(0.13)	12.89(0.13)	13.01(0.39)
Fe_2O_3	6.65(0.03)	14.52(0.03)	13.12(0.24)	15.52(0.08)	8.65(0.25)	8.05(0.36)	15.91(0.11)	7.79(0.08)	7.04(0.10)
FeO	8.83(0.03)	0.40(0.03)	1.60(0.22)	0.00(0.07)	3.49(0.25)	5.96(0.35)	0.00(0.10)	8.60(0.07)	10.50(0.09)
MnO	0.88(0.03)	0.55(0.00)	0.71(0.03)	1.74(0.01)	0.26(0.01)	0.71(0.03)	3.60(0.12)	3.62(0.01)	3.52(0.03)
MgO	0.52(0.05)	0.94(0.01)	1.11(0.14)	1.28(0.05)	<0.002	<0.002	0.70(0.02)	0.68(0.04)	0.76(0.05)
CaO	8.55(0.03)	13.08(0.15)	11.90(0.13)	9.34(0.11)	20.93(0.25)	12.29(0.30)	7.49(0.06)	7.57(0.04)	9.19(0.04)
Sc_2O_3	<0.002	<0.002	<0.002	<0.002	<0.002	<0.002	<0.002	<0.002	<0.002
Y_2O_3	<0.10	<0.10	<0.10	<0.10	2.30(0.27)	<0.10	1.00(0.01)	0.80(0.05)	0.77(0.04)
La_2O_3	6.79(0.08)	3.98(0.02)	4.51(0.13)	5.26(0.05)	<0.11	3.26(0.05)	3.23(0.02)	4.12(0.04)	3.90(0.10)
Ce_2O_3	12.98(0.06)	6.60(0.05)	7.41(0.07)	8.62(0.12)	0.22(0.04)	8.20(0.37)	7.13(0.04)	8.34(0.10)	8.33(0.08)
Pr_2O_3	1.42(0.01)	1.09(0.07)	1.20(0.04)	1.27(0.05)	<0.13	1.67(0.06)	1.25(0.09)	1.40(0.04)	1.44(0.03)
Nd_2O_3	3.13(0.00)	3.15(0.02)	3.21(0.05)	3.87(0.07)	0.51(0.07)	5.19(0.07)	4.22(0.05)	4.32(0.03)	4.56(0.07)
Sm_2O_3	0.77(0.05)	0.67(0.02)	0.70(0.06)	0.73(0.01)	0.71(0.03)	1.06(0.03)	1.24(0.01)	1.12(0.01)	1.37(0.04)
Gd_2O_3	<0.22	0.41(0.03)	0.48(0.06)	0.57(0.04)	1.03(0.01)	0.71(0.01)	1.17(0.05)	1.04(0.10)	1.19(0.03)
Tb_2O_3	<0.15	<0.15	<0.15	<0.15	<0.15	<0.15	<0.15	<0.15	<0.15
Dy_2O_3	<0.22	0.32(0.04)	0.40(0.05)	0.42(0.01)	0.50(0.06)	0.26(0.02)	<0.22	<0.22	<0.22
Er_2O_3	<0.13	<0.13	<0.13	<0.13	<0.13	<0.13	<0.13	<0.13	<0.13
Tm_2O_3	<0.12	<0.12	<0.12	<0.12	<0.12	<0.12	<0.12	<0.12	<0.11
Yb_2O_3	<0.11	<0.11	<0.11	<0.11	<0.11	<0.11	<0.11	<0.11	<0.11
ThO_2	1.66(0.03)	1.37(0.05)	2.08(0.10)	1.30(0.10)	<0.01	<0.01	2.63(0.04)	2.30(0.08)	1.70(0.05)
Na_2O	<0.04	<0.04	<0.04	<0.04	<0.04	<0.04	<0.04	<0.04	<0.04
K_2O	<0.01	<0.01	<0.01	<0.01	<0.01	<0.01	<0.01	<0.01	<0.01
Total	98.87	101.63	100.00	101.85	99.90	98.99	97.77	97.81	100.03
Si	2.997(0.007)	3.034(0.066)	2.946(0.169)	3.087(0.100)	3.046(0.042)	3.062(0.060)	3.068(0.030)	3.053(0.111)	2.976(0.015)
^{T}Al	0.003(0.000)	0.000	0.054(0.000)	0.000	0.000	0.000	0.000	0.000	0.024(0.000)
Total *T*	3.000	3.034	3.000	3.087	3.046	3.062	3.068	3.053	3.031
Ti	0.080(0.079)	0.036(0.003)	0.046(0.007)	0.038(0.001)	0.018(0.004)	0.056(0.017)	0.134(0.004)	0.119(0.005)	0.110(0.003)
^{M}Al	1.649(0.031)	1.850(0.035)	1.810(0.116)	1.666(0.020)	2.180(0.061)	1.825(0.087)	1.462(0.027)	1.469(0.063)	1.439(0.064)
Fe^{3+}	0.483(0.015)	0.932(0.016)	0.878(0.023)	1.024(0.006)	0.522(0.030)	0.550(0.066)	1.114(0.014)	0.567(0.044)	0.505(0.028)
Fe^{2+}	0.713(0.015)	0.029(0.017)	0.119(0.025)	0.000(0.007)	0.234(0.030)	0.452(0.066)	0.000(0.016)	0.695(0.049)	0.837(0.031)
^{M}Mn	0.000	0.000	0.000	0.017(0.000)	0.000	0.055(0.006)	0.125(0.000)	0.000	0.000
Mg	0.075(0.014)	0.119(0.001)	0.147(0.038)	0.167(0.010)	0.000	0.000	0.097(0.007)	0.098(0.024)	0.109(0.015)
Total *M*	3.000	2.966	3.000	2.913	2.954	2.938	2.932	2.948	3.000
Ca	0.884(0.012)	1.195(0.049)	1.134(0.064)	0.877(0.033)	1.799(0.038)	1.195(0.052)	0.747(0.009)	0.784(0.029)	0.939(0.014)
^{A}Mn	0.072(0.007)	0.040(0.000)	0.054(0.005)	0.112(0.000)	0.017(0.018)	0.000	0.158(0.018)	0.296(0.008)	0.284(0.007)
Sc	0.000	0.000	0.000	0.000	0.000	0.000	0.000	0.000	0.000
Y	0.000	0.000	0.000	0.000	0.098(0.024)	0.000	0.050(0.001)	0.041(0.005)	0.039(0.004)
La	0.242(0.005)	0.125(0.004)	0.148(0.003)	0.170(0.001)	0.000	0.109(0.002)	0.111(0.003)	0.147(0.002)	0.137(0.009)
Ce	0.459(0.003)	0.206(0.001)	0.241(0.007)	0.277(0.003)	0.006(0.002)	0.272(0.028)	0.243(0.002)	0.295(0.013)	0.291(0.009)
Pr	0.050(0.008)	0.034(0.005)	0.039(0.004)	0.041(0.002)	0.000	0.055(0.005)	0.042(0.006)	0.049(0.003)	0.050(0.002)
Nd	0.108(0.000)	0.096(0.000)	0.102(0.001)	0.121(0.003)	0.015(0.004)	0.168(0.006)	0.140(0.003)	0.149(0.006)	0.155(0.002)
Sm	0.026(0.001)	0.020(0.001)	0.021(0.004)	0.022(0.001)	0.019(0.002)	0.033(0.002)	0.040(0.001)	0.037(0.002)	0.045(0.003)
Gd	0.000	0.012(0.001)	0.014(0.004)	0.017(0.002)	0.031(0.000)	0.021(0.001)	0.036(0.003)	0.033(0.007)	0.038(0.001)
Tb	0.000	0.000	0.000	0.000	0.000	0.000	0.000	0.000	0.000
Dy	0.000	0.009(0.002)	0.011(0.003)	0.012(0.000)	0.015(0.004)	0.008(0.002)	0.000	0.000	0.000
Er	0.000	0.000	0.000	0.000	0.000	0.000	0.000	0.000	0.000
Tm	0.000	0.000	0.000	0.000	0.000	0.000	0.000	0.000	0.000
Yb	0.000	0.000	0.000	0.000	0.000	0.000	0.000	0.000	0.000
Th	0.036(0.002)	0.027(0.002)	0.042(0.004)	0.026(0.004)	0.000	0.000	0.056(0.001)	0.051(0.002)	0.037(0.002)
Na	0.000	0.000	0.000	0.000	0.000	0.000	0.000	0.000	0.000
K	0.000	0.000	0.000	0.000	0.000	0.000	0.000	0.000	0.000
Total *A*	1.877	1.764	1.806	1.675	2.000	1.861	1.623	1.882	2.015

See Figures 1j–m for spot locations. * According to the definition used by Pan & Fleet (1991), allanite requires at least 50% occupancy of the *A*2 site by total rare-earth elements (REE), corresponding to 15 wt%. Therefore, the data on the sample from Hirono in column 1* pertain to REE-rich epidote. *n*: number of microprobe points. Number in parentheses is standard deviation. The compositions are first reported in wt%, then the proportion of cations is reported in atoms per formula unit (*apfu*).